SINTEF
PROCEEDINGS
2

Proceedings of the 12th International Conference on Computational Fluid Dynamics in the Oil & Gas, Metallurgical and Process Industries

Progress in Applied CFD – CFD2017

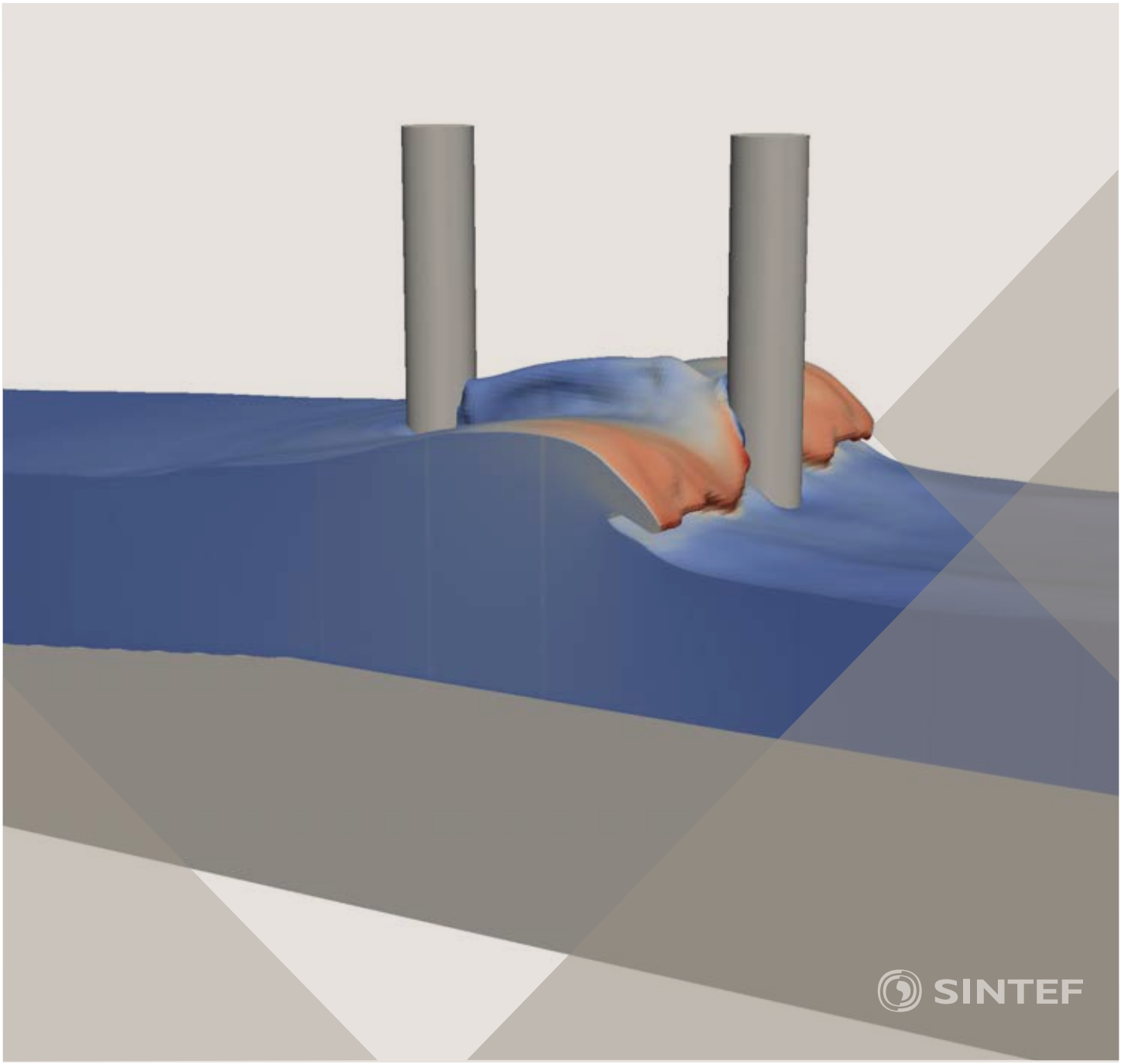

SINTEF Proceedings

Editors:
Jan Erik Olsen and Stein Tore Johansen

Progress in Applied CFD – CFD2017

Proceedings of the 12th International Conference on Computational Fluid Dynamics in the Oil & Gas, Metallurgical and Process Industries

SINTEF Academic Press

SINTEF Proceedings no 2
Editors: Jan Erik Olsen and Stein Tore Johansen
Progress in Applied CFD – CFD2017
Selected papers from 10th International Conference on Computational Fluid Dynamics in the Oil & Gas, Metallurgical and Process Industries

Key words:
CFD, Flow, Modelling

Cover, illustration: Arun Kamath

ISSN 2387-4295 (online)
ISBN 978-82-536-1544-8 (pdf)

SINTEF Academic Press
Address: Forskningsveien 3 B
PO Box 124 Blindern
N-0314 OSLO
Tel: +47 73 59 30 00
Fax: +47 22 96 55 08

www.sintef.no/byggforsk
www.sintefbok.no

SINTEF Proceedings
SINTEF Proceedings is a serial publication for peer-reviewed conference proceedings on a variety of scientific topics.
The processes of peer-reviewing of papers published in SINTEF Proceedings are administered by the conference organizers and proceedings editors. Detailed procedures will vary according to custom and practice in each scientific community.

PREFACE

This book contains all manuscripts approved by the reviewers and the organizing committee of the 12th International Conference on Computational Fluid Dynamics in the Oil & Gas, Metallurgical and Process Industries. The conference was hosted by SINTEF in Trondheim in May/June 2017 and is also known as CFD2017 for short. The conference series was initiated by CSIRO and Phil Schwarz in 1997. So far the conference has been alternating between CSIRO in Melbourne and SINTEF in Trondheim. The conferences focuses on the application of CFD in the oil and gas industries, metal production, mineral processing, power generation, chemicals and other process industries. In addition pragmatic modelling concepts and bio-mechanical applications have become an important part of the conference. The papers in this book demonstrate the current progress in applied CFD.

The conference papers undergo a review process involving two experts. Only papers accepted by the reviewers are included in the proceedings. 108 contributions were presented at the conference together with six keynote presentations. A majority of these contributions are presented by their manuscript in this collection (a few were granted to present without an accompanying manuscript).

The organizing committee would like to thank everyone who has helped with review of manuscripts, all those who helped to promote the conference and all authors who have submitted scientific contributions. We are also grateful for the support from the conference sponsors: ANSYS, SFI Metal Production and NanoSim.

Stein Tore Johansen & Jan Erik Olsen

Organizing committee:

Conference chairman: Prof. Stein Tore Johansen
Conference coordinator: Dr. Jan Erik Olsen
Dr. Bernhard Müller
Dr.Sigrid Karstad Dahl
Dr.Shahriar Amini
Dr.Ernst Meese
Dr.Josip Zoric
Dr.Jannike Solsvik
Dr.Peter Witt

Scientific committee:

Stein Tore Johansen, SINTEF/NTNU
Bernhard Müller, NTNU
Phil Schwarz, CSIRO
Akio Tomiyama, Kobe University
Hans Kuipers, Eindhoven University of Technology
Jinghai Li, Chinese Academy of Science
Markus Braun, Ansys
Simon Lo, CD-adapco
Patrick Segers, Universiteit Gent
Jiyuan Tu, RMIT
Jos Derksen, University of Aberdeen
Dmitry Eskin, Schlumberger-Doll Research
Pär Jönsson, KTH
Stefan Pirker, Johannes Kepler University
Josip Zoric, SINTEF

CONTENTS

GRANULAR FLOW DESCRIBED BY FICTITIOUS FLUIDS: A SUITABLE METHODOLOGY FOR PROCESS SIMULATIONS

Manuel SPARTA*, **Svenn Anton HALVORSEN**

Teknova AS, 4612 Kristiansand, NORWAY

* E-mail: manuel.sparta@teknova.no

ABSTRACT

The flow of granular materials is often present in metallurgical reactors. Metallurgical simulations are typically multidisciplinary and the granular flow will often have a significant effect on the temperature distribution. The flow of bulk materials exhibits patterns that can be very different from fluid flows. Standard fluid flow methods are not applicable to describe such flows.

For simple bulk flows with plug flow sections and mass flow hoppers, a reasonable flow field can, however, be computed with a standard CFD tool. The trick is to apply appropriate, non-standard, moving wall boundary conditions.

This simple approach does not work for complex flow cases, including sections with one or more free boundaries. For such cases, we apply the Discrete Element Method (DEM), which has emerged to be the preferred choice for simulation of granular flow. A suitable method has been developed to compute the volume averaged flow field by DEM and then import it into a code for multiphysics simulations.

To reduce the high computational cost of DEM simulations a hybrid approach is recommended. DEM simulations are then used for the complex flow regions while the simple model is used wherever applicable. In the multiphysics program the flow field is forced to be equal, or very close to, the DEM results by applying a suitable volume force.

Keywords: Granular flow, Fictitious fluids, Standard CFD software, Process metallurgy.

NOMENCLATURE

Φ	Total flow, [m^3/s]
Ω	Cross section, [m^2]
a	Characteristic length, [m]
z	Vertical coordinate, [m]
$\mathbf{u}$	Velocity, [m/s]
$\overline{w}(z)$	Average vertical velocity, [m/s]
u	radial component of the velocity, [m/s]
w	vertical component of the velocity, [m/s]
K	Force factor, [Ns/m^4]
s_Φ	Total flow scaling factor, [1]

INTRODUCTION

The flow of granular material is ubiquitous in metal production with the transport of ores and carbonaceous materials in furnaces being a primary example. Granular flows exhibit patterns that can be very different from fluid flows (Jenike, 1964). For example, arc formation can clog outlets, small change in the hopper angle may result in the transition from funnel flow (with stagnant areas) to mass flow (with flow in the whole cross section). If obstacles are present, upstream stagnant zones and empty cavities downstream are easily formed. All these effects can sum up counterintuitively, to the extent that the placement of obstacles can increase the flow rate (obstacles are routinely inserted before outlet opening in silos). These unique features imply that standard fluid models do not provide good approximations to granular flow. Significant efforts have been spent to derive numerical models for granular materials (for a recent review we refer to the work of Tang et al. (2015)), but such methods may not be implemented in common multiphysics programs.

Metallurgical simulations are typically multidisciplinary and the granular flow will often have a significant effect on the temperature distribution. For many applications, the general flow patterns are essential, while details can be neglected. It is most convenient if these patterns can be available within the computational tool you normally apply for multidisciplinary simulations.

We follow the the spirit of application-driven pragmatic modeling, i.e. deriving simplest possible model which can give fast, and sufficiently accurate answers (c.f. Zoric et al. 2014). We started to test whether standard CFD tools might be suitably adapted, to describe granular flow.

This article is organized as follows, a fictitious model geometry showing some challenges of a metallurgic reactor is presented. In first approximation, we attempt to enforce a granular-like flow applying available boundary conditions. Secondly, we show how to derive a template flow using Discrete Element Methods simulations and import it into a Multiphysics environment. Finally, we discuss the capabilities of a hybrid approach. All our testing is done in COMSOL Multiphysics (COMSOL, 2016), which is the tool that we routinely use.

Model Geometry

After some initial trials, we chose to test our ideas on an axially symmetric geometry shown in Figure 1. This geometry is not based on any real reactor, but was designed to test some common patterns for granular flow:

a) A straight section at the top where plug flow is expected
b) A mass flow hopper
c) Another straight section with plug flow
d) A sharp widening of the domain where there will be a free surface, given by the angle of repose for the bulk material.
e) Stagnant (non-moving) particles on top of an obstacle (grey section)
f) A cavity just beneath the obstacle

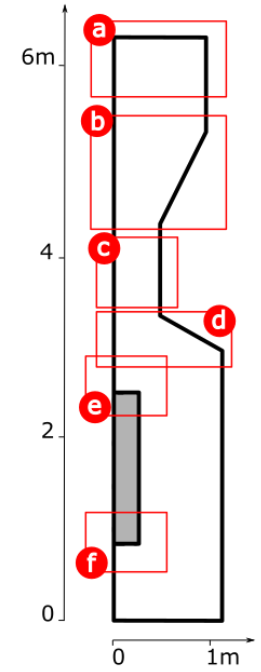

Figure 1: Geometry of the cylindrical model investigated. Areas of interest are highlighted: a) Plug flow zone b) Mass flow hopper c) Plug flow zone d) Abrupt widening with a free surface e) Stagnant particles on top of an obstacle f) Cavity right underneath the obstacle.

SIMULATIONS

Simple adaptation of viscous flow

First we considered the upper part of our test reactor, consisting of sections a), b), and c). The flow here is comparatively simple with plug flow in a) and c) and a velocity gradient in b).

For our case, we set the velocity in the hopper center to be roughly twice as big as at the wall. This seems realistic for particulate flow (Jenike, 1964). Further, a parabolic velocity profile seems reasonable here. Hence, the flow field in b) should be properly described by viscous laminar flow.

We then applied boundary conditions to achieve the desired flow patterns for the upper sections.

For the vertical walls, there are two options:

1) *Slip* condition – Wall without friction. The flow is only forced to move parallel to the wall.
2) *No slip* and a *moving wall* with a prescribed vertical velocity, given by the plug flow requirement. The viscous fluid will then match the velocity of the wall.

For a long straight section of fluid domain, the 2 approaches show the same result, plug flow. We favor, however, the second option as the boundary condition then plays an active role near geometrical transitions.

For the hopper section, we again rely on the moving wall condition. The first step is to compute the average vertical velocity as a function of the z-coordinate.

$$-\overline{w}(z)=\frac{\Phi}{\Omega(z)} \qquad (1)$$

where Φ is the total flow, and $\Omega(z)$ is the horizontal cross section area.

Then, we let the vertical velocity at the wall be equal to the average velocity scaled by a suitable factor, in our case 2/3 worked well. An appropriate radial component is set to ensure that the flow is parallel to the wall, hence the wall velocity at the hopper wall is equal to:

$$\mathbf{u}_f=\left[-2\frac{\overline{w}(z)}{3},-2\frac{\overline{w}(z)}{3}\tan(\alpha)\right] \qquad (2)$$

where α is the hopper angle.

The flow field obtained with this setup is shown in Figure 2, where the total flow rate is set to 1 m^3/h. The first panel shows the radial component of the flow velocity and, as expected, this is zero except in the hopper. The vertical component has a flat profile in the zones a) and c) as described by the plug flow and the acceleration occurs in the hopper.

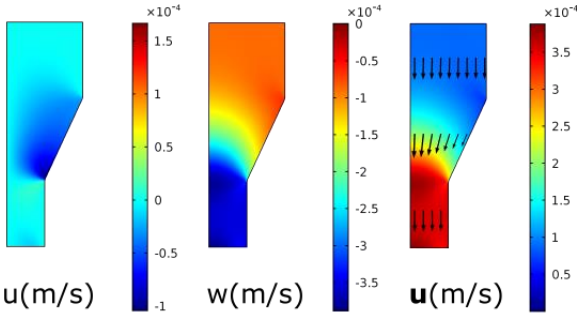

Figure 2: Top section of the model system, flow obtained imposing "No Slip condition" and prescribed wall velocities.

The simple approach gives a realistic particulate flow field. A fictitious fluid flow is computed as the boundary conditions are not realistic for viscous flow.

For a given geometry it is sufficient with one CFD computation. If the results for another value of the total flow is required, the computed velocities are simply multiplied with the appropriate factor, to get the correct total flow. Granular flow is gravity driven and does not change pattern significantly as long as the motion is sufficiently small, i.e. inertia effects can be neglected.

Flow at a free boundary

While laminar viscous flow worked well with adapted boundary conditions, this approach failed to describe the conditions at the free boundary in region d). At the free surface, there will be a thin layer, a few particle diameters thick, where the particles will move at a comparatively high speed (Shinohara, 1987 and Williams, 1976). Below this layer, the bulk velocity will be much slower. Such sharp change in the fluid velocity cannot be described by simply adapting the boundary conditions for a viscous fluid.

We tried to add one or more inner walls to enforce a suitable boundary layer at the free surface, but were not able to adapt a reasonable bulk flow pattern. We cannot preclude that such a procedure may succeed, but based on our trials, it does not look promising.

Application of Discrete Element Model (DEM)

To obtain an accurate description of the problematic areas d)-f) we turn to the use of a Discrete Element Method simulations.

The Discrete Element Method (DEM) was first introduced by Cundall and Strack (1979) and in recent years, thanks to increasing of computational power and the development of efficient programs, it has become wildly used to investigate granular flow. In a nutshell, DEM predicts the bulk properties of a granular flow by analyzing the time propagation of position and momentum of each individual particle. Each particle is represented by a simple and well defined geometrical entity in most cases a sphere. The translational and angular accelerations are computed as the result of the corresponding momentum balances (Ariyama et al., 2014; Guo and Curtis, 2015). Realistic simulations involve, however, a huge number of particles and the computational time may be correspondingly high. Furthermore, the method can be appropriate to obtain the flow patterns, but it is unsuitable to include in multidisciplinary iterations. For the latter case, our special application of standard CFD software is clearly preferable.

For our case, the workflow is organized as follows:

- Set up and run a DEM simulation for a suitable 3D model of the system under investigation, c.f. Appendix A.
- By means of space and time averaging, turn the information of the DEM snapshots into a discretized flow field (Appendix B).
- Import the computed flow field into COMSOL Multiphysics.

The detailed description of the DEM simulation can be found in Appendix A. Briefly, the 3D model for the system of interest is constructed starting from the 2D axisymmetric model. Auxiliary structural elements functional to the keep the operation during the DEM simulation steady (see Figure 3) are added. In this case, a sufficiently large reservoir of particles was introduced above section a), to ensure particles flowing uniformly into our test reactor. A hopper section was applied, but a cylindrical region could alternatively have been chosen. The lower part was extended and a flat plate was introduced. This plate was lowered at a constant speed, to control the gravity driven flow. The vertical velocity at the bottom was set to 0.01 m/s. This seems like an unreasonable high flow, but as already stated: the flow patterns do not depend on the speed, as long as inertia effect can be neglected.

A 200 s simulation time was applied and a snapshot of the system was taken every 0.04 s. Each snapshot contains for each particle its Cartesian coordinates, radius and velocity in Cartesian components.

The free surface is clearly visible in Figure 3. The model also showed a void beneath the obstacle, section f). This void is not visible as the figure is in 3D, i.e. just beneath the obstacles we see the particles behind the void.

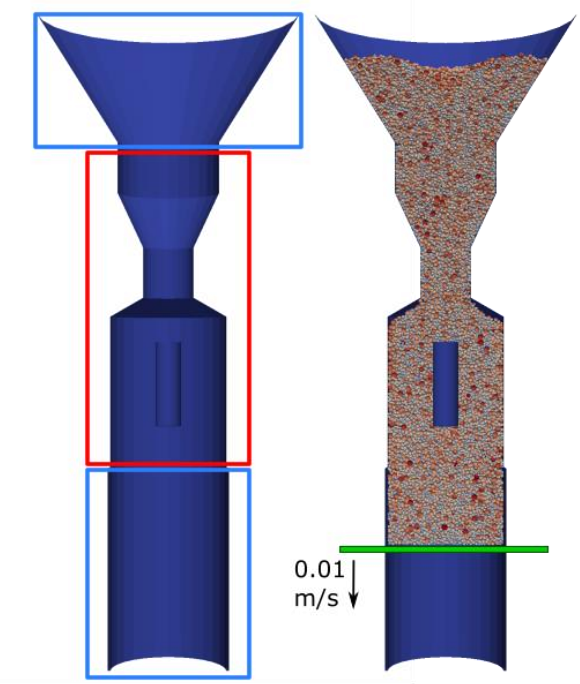

Figure 3: Left side: 3D model of the reactor walls. The original area of interest is highlighted with a red box. Auxiliary feeder and output sections are marked with light blue. Right: Snapshot of the DEM simulation.

After a sufficiently long simulation, the information collected in the snapshots are transformed into a suitable flow field. Details of this steps are given in Appendix B. Briefly, for one snapshot, particle velocities in 3D space are projected into a fine grid (grid elements smaller than the particles) in a 2D subdomain as shown in Figure 4 (space average). Subsequently, the information from several snapshots is combined (time average) and this greatly reduces the granularity of the field as seen in Figure 4.

The time average results are adjusted to ensure that the flow is correct at each level and smoothed using convolutions with a 5x5 Gaussian kernel (Davies, 1990) as shown in Figure 5.

The result of the procedure is shown in Figure 6 were the radial and vertical component of the flow velocity are depicted. Both components have the expected characteristics, the radial term vanishes in all the straight

sections and it assumes relatively large values only at the widening of the domain in the d) zone.

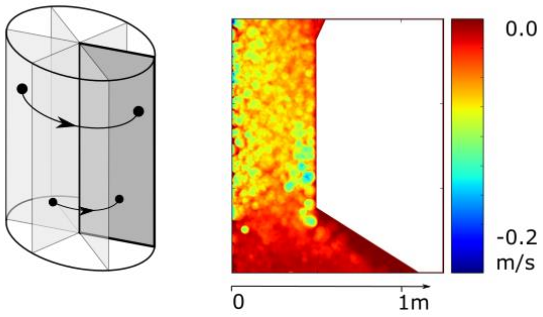

Figure 4: Left: The particles on the 3D DEM model are projected into a grid in the 2D subspace. Right: Details of the projection of one DEM snapshot.

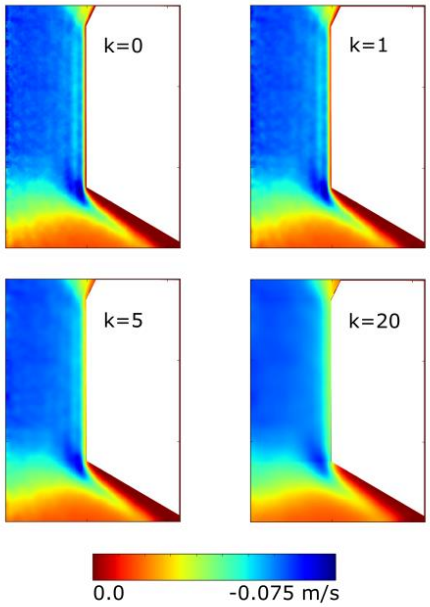

Figure 5: Detail of the vertical component of the flow field, smoothing with Gaussian convolution. Effect of subsequent applications (k) of the filter.

The voids in sections d) and f) are shown as regions of zero velocities. Observe that the highest velocity is not shown at the free surface in zone d), but slightly below. At the free surface, the particles will flow at the highest velocity. We have, however, computed the average volume flow. Since there are fewer particles found *at* the free boundary than *slightly below*, the average volume flow is diminished very close to the boundary. Further, the center of the particles will always be at least one radius away from the void region. Hence, moving towards the free boundary, a smaller and smaller fraction of a particle can be present. The average volume velocity will then gradually be lowered and reaching zero at the boundary. This latter effect also causes the average velocity to approach zero at any boundary, c.f. Figure 5 for k = 0. A stagnant zone is visible in the vertical component of the velocity in the e) zone.

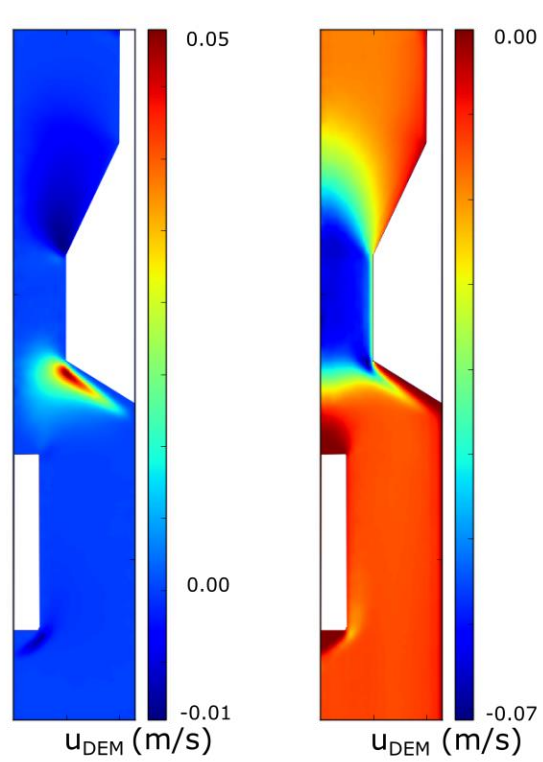

Figure 6: Components of the velocity field extracted from a DEM simulation. Left: radial component, Right: vertical component.

The data are saved in a text file that can be imported via the interpolated function feature of COMSOL. Here, after re-scaling with the appropriate total flow, the velocities can be natively used in multiphysics applications.

Having the fictitious fluid velocities obtained with DEM it is interesting to evaluate the performance of the approach based on wall speeds. The flows, apart from a scaling factor due to the higher DEM flow, are qualitatively similar (see Figure 2 and Figure 6). The only obvious difference is that with DEM one always obtains a boundary effect near walls whereas the simple approach gives a homogeneous velocity profile. Since the total flow is exact in both cases, the simple approach overestimates the fluid velocities near the boundaries (approximately 2-3 particle radiuses) and slightly underestimate elsewhere.

Hybrid approach

In the previous section, we demonstrated how to construct and analyze a DEM simulation to obtain a bulk flow field that can be used within COMSOL. An obvious disadvantage is that the DEM simulation can be costly in terms of resources and computational time when applied to metallurgical systems. One possible solution is to use the DEM approach only for the zones that are foreseen to be problematic. In the example considered in this work, an experienced practitioner may realize that the section comprising the zones d) and e) and the region including zone f) require DEM treatment. An *ad hoc* sub-model can then be extracted and treated with the outlined DEM procedure (see Figure 7). We found that the smaller DEM model only required half the simulation time.

Once the DEM simulation is processed as described above, the resulting flow field is mapped back into the original geometry and it is used as a "flow template". Within the two applicable regions we add a volume force that will force the flow to be equal, or very close to the DEM flow field. We applied stationary simulation and a proportional controller, that is we used the volume forces:

$$F_r(r,z) = K(s_\Phi u_{DEM} - u) \quad (3)$$

$$F_z(r,z) = K(s_\Phi w_{DEM} - w) \quad (4)$$

where u_{DEM}, and w_{DEM} are the velocity components from DEM, K is a suitable large number and s_Φ is the scaling factor to ensure that the DEM total flow matches the CFD simulation. Other methods can be applied.

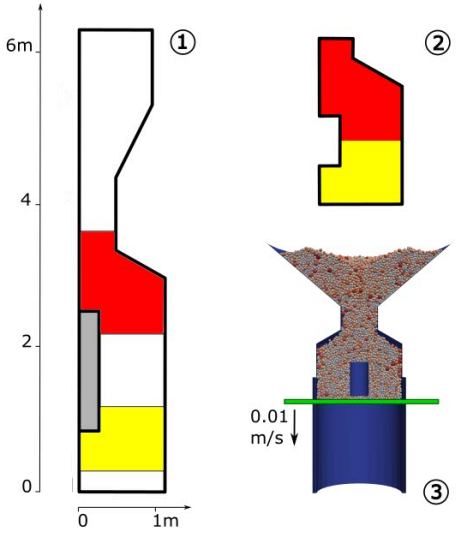

Figure 7: 1) Problematic sections of the system are identified. 2) A subsystem is constructed. 3) Snapshot of the DEM simulation.

To avoid discontinuities, we recommend the use of a smoothing function in the transition between forced (velocities from DEM) and free zones.

The results of the hybrid procedure are shown in Figure 8 where the velocity components of the fictitious fluid flow are shown. These are in excellent agreement with the DEM results of Figure 6 (apart from a scaling factor since the DEM simulation have applied a higher flow).

In this example, the complexity/cost of the DEM calculation is reduced by only a factor of 2. While this may not justify the use of a hybrid approach, it demonstrates that complex systems can be partitioned in subdomains to be solved individually. A model can then be incrementally improved by adding subsequent sections where flow velocities are DEM-derived.

There are small details that the approach cannot cover. For example, the simplified approach imposes a uniform velocity across any cross section of any straight domain. This is in contrast with the DEM results that predict a small boundary effect at the walls. As explained above, the velocity will approach zero at any (non-moving) boundary. For this reason, at the transition between the forced and free zones, small artefacts in the fluid flow can occur.

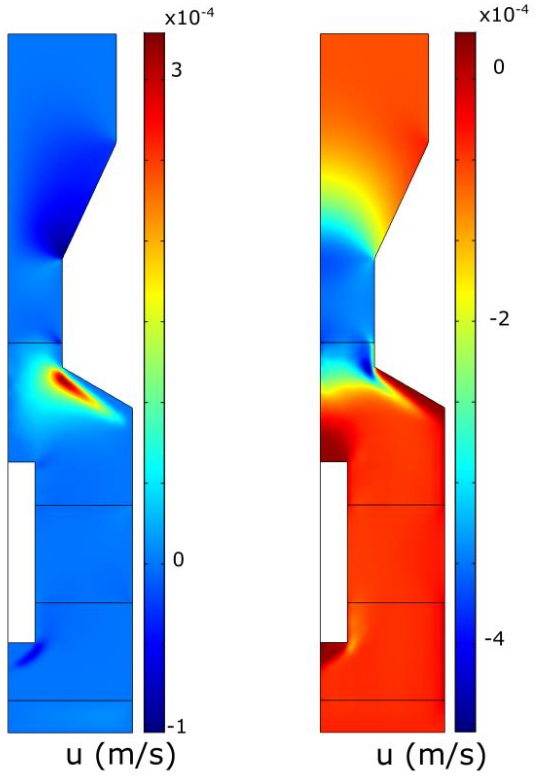

Figure 8: Components of the velocity field extracted from a DEM simulation.

CONCLUSIONS

For comparatively simple bulk flow like plug flow sections and mass flow hoppers, a reasonable flow field can be computed applying viscous laminar flow with appropriate moving wall boundary conditions.

This simple approach does not work for more complex flows, e.g. regions with a free boundary. The flow field must then be found by other methods, for instance a DEM simulation.

A suitable method has been developed to average DEM results and import the flow field into a program for Multiphysics simulations.

To reduce the computational cost of DEM simulations a hybrid approach is recommended. DEM simulations are then used for the complex flow regions while the simple model is used wherever applicable.

REFERENCES

ARIYAMA, T., NATSUI, S., KON, T., UEDA, S., KIKUCHI, S., NOGAMI, H., (2014) "Recent Progress on Advanced Blast Furnace Mathematical Models Based on Discrete Method." *ISIJ International*, **54,** 1457-1471.

CUNDALL, P.A. and STRACK, O.D.L., (1979), "A discrete element model for granular assemblies", *Geotechnique*, **29**, 47-65.

COMSOL Multiphysics® v.5.2a. (2016) www.comsol.com. COMSOL AB, Stockholm, Sweden.

DAVIES, E., (1990), "Machine Vision: Theory, Algorithms and Practicalities", Academic Press, 42-44.

GUO, Y., CURTIS, J.S., (2015) "Discrete Element Method Simulations for Complex Granular Flows", *Annu. Rev. Fluid Mech.,* **47**, 21-46.

KLOSS, C., GONIVA, C., HAGER, A., AMBERGER, S., PIRKER, S., (2012), "Models, algorithms and validation for opensource DEM and CFD-DEM", *Prog. Comput. Fluid Dy.*, **12**, 140-152.

JENIKE, A.W., (1964), "Storage and Flow of Solids", Bulletin 123, University of Utah Engineering Station, USA.

NATSUI, S., UEDA, S., FAN, Z., ANDERSSON, N., KANO, J., INOUE, R., ARIYAMA, T., (2009), "Characteristics of Solid Flow and Stress Distribution Including Asymmetric Phenomena in Blast Furnace Analyzed by Discrete Element Method", *ISIJ International,* **50**, 207-214.

SAKAI, M., ABE, M., SHIGETO, Y., MIZUTANI, S., TAKAHASHI, H., VIRE, A., PERCIVAL, J., XIANG, J., PAIN, C., (2016), "Verification and validation of a coarse grain model of the DEM in a bubbling fluidized bed", *Chem Eng J*, **244**, 33-43.

SHINOHARA, K., (1987), "General Mechanism of Particle Segregation during Filling Hoppers", Proceedings of 9th CHISA Congress, section H: Particulate Solids, H.3.5, Prague.

TANG, Y., ZHANG, L., GUO, Q., (2015), "A review on numerical models for granular flow inside hoppers and its applications in PBR", *J. Nucl. Sci. Technol.,**52,*** 759-768.

WILLIAMS, J.C., (1976), "The segregation of particulate materials", *Powder Technol.*, **15**, 245-256.

ZORIC, J., JOHANSEN, S.T., EINARSRUD, K.T. SOLHEIM, A., (2014) "On pragmatism in industrial modeling," in CFD 2014 - 10th International Conference on Computational Fluid Dynamics in the Oil & Gas, Metallurgical and Process Industries, Trondheim, 1–16.

APPENDIX A – DEM CALCULATION

The descriptions of complex flow zones in the granular flow calls for the use of DEM simulations. The first step in this endeavor is the construction of a 3D mesh. Having the 2D axisymmetric projection of the fluid domain already implemented in COMSOL greatly simplifies this operation and the 3D model of the wall is obtained by revolving the trace of the fluid domain, obtaining a volume of approximately 19 m^3. At this stage, the 3D model should be equipped with a feeder zone and output zone designed to keep the flow steady and control with precision the flux. These two features are shown in the left panel of Figure 3. The DEM simulation was carried out using LIGGGHTS® (Kloss et al., 2012). The particles have density equal to 1000 kg/m^3 and a radius normally distributed around the mean value 3 cm (standard deviation 1 cm). The granular model "Hertz" was used to compute the frictional force between two granular particles; the evolution of the tangential overlap during particles - particle contact is used to modify the spring part of the tangential. Finally, an additional torque contribution is added via the epsd2 rolling friction model. The following material properties and interactions were used for the simulation: Young's modulus $4.7*10^9$ Pa; Poisson's ratio 0.35; coefficient of restitution 0.43; coefficient of friction 0.73, coefficient of rolling friction 0.21. The time step was set to 10^{-5} s. The right panel of Figure 3 depicts a snapshot of the DEM simulations with the system loaded with approximately 134000 spherical particles. While this number of particles is representative of an industrial application using rather lumpy material, DEM simulations employing large particles are common in the field (see e.g. Natsui et al., 2009) and Corse Grain approximations are emerging as a viable tool to reduce computational costs (Sakai, 2016). After equilibration of the loaded particles, 200 s simulation was performed and a snapshot was saved every 4000 time steps. During this time the wall at the bottom of the system was moving downward at a constant speed of 0.01 m/s, corresponding to a flow of $4.2*10^{-2}$ m^3/s. These values exceed normal metallurgical operational conditions but ensures that each particle travels enough space to be able to collect a representative picture with a relative short simulation. For reference, the DEM calculations took approximately 4 days on a standard desktop PC.

APPENDIX B – HOMOGENEIZATION

This appendix describes the transformation of the information collected in the DEM snapshots into the flow field of a fictitious fluid.

The first step to be accomplished is the space averaging as depicted in Figure 4. In practice, the Cartesian coordinates and velocity components for each particle are transformed in cylindrical coordinates and projected into the 2D subspace of the axisymmetric model. The projection occurs over a discretized grid whose elements are smaller than the particles. The space average takes into consideration both the volume of the particle and the total volume extruded over the projection itself.

A detail of the outcome of the space average is shown in the right panel of Figure 4 where the magnitude of the vertical component of the velocity is rendered. Although the space averaging successfully collects all the information of the 3D model and translated it into a bidimensional field component, the granular nature of the system is still evident and "shadows" of the individual particles are still visible.

The second step consists of combining data from several snapshots into a time average. In the specific case, we used 450 snapshots collected every 0.4 s in the range 20-200 s of the DEM simulation.

At this stage, it is important to realize that the approach so far does not include the movement of the "empty" fraction of the bulk. A possible solution is to scale all the velocities with a factor inversely proportional to the packing density of the system. Alternatively, the bulk flux (imposed in the DEM simulation), can be used to scale the flux for each row of the grid in the 2D subspace. An example of the results at this stage is shown in the top left section of Figure 5. Although the flux of the fictitious fluid is now exact by design, some noise is still present in the flow fields and small artefacts emerge near the walls (see vertical striations in Figure 5). This can be corrected using a smoothing function. Here we use repeated convolutions with a 5x5 Gaussian kernel (Davies, 1990).

The operations described in this section refer to a 2D axisymmetric COMSOL simulation. However, only small modifications of the projection function and smoothing procedure are needed to address Cartesian 2D and full 3D cases.